BMC Biology

RESEARCH ARTICLE

Open Access

A mucus layer derived from porcine intestinal organoid air–liquid interface monolayer attenuates swine enteric coronavirus infection by antiviral activity of Muc2

Ning Yang[1,2,3†], Yang Li[1,3†], Yifei Cai[1,3,4], Yuanyuan Liu[1,3,5], Yunhang Zhang[1,2,3], Yuguang Fu[1], Chen Tan[1,2,3], Luc Willems[2] and Guangliang Liu[1,3,5*]

Abstract

Background The mucus layer provides the first defense that keeps the epithelium free from microorganisms. However, the effect of the small intestinal mucus layer on pathogen invasion is still poorly understood, especially for swine enteric coronavirus. To better understand virus–mucus layer–intestinal epithelium interactions, here, we developed a porcine intestinal organoid mucus–monolayer model under air–liquid interface (ALI) conditions.

Results We successfully established a differentiated intestinal organoid monolayer model comprising various differentiated epithelial cell types and a mucus layer under ALI conditions. Mass spectrometry analysis revealed that the mucus derived from the ALI monolayer shared a similar composition to that of the native small intestinal mucus. Importantly, our results demonstrated that the ALI monolayer exhibited lower infectivity of both TGEV and PEDV than did the submerged monolayer. To further confirm the impact of ALI mucus on coronavirus infection, mucus was collected from the ALI monolayer culture system and incubated with the viruses. These results indicated that ALI mucus treatment effectively reduced the infectivity of TGEV and PEDV. Additionally, Mucin 2 (Muc2), a major component of native small intestinal mucus, was found to be abundant in the mucus derived from the ALI monolayer, as determined by mass spectrometry analysis. Our study confirmed the potent antiviral activity of Muc2 against TGEV and PEDV infection. Considering the sialylation of Muc2 and the known sialic acid-binding activity of coronavirus, further investigations revealed that the sialic acid residues of Muc2 play a potential role in inhibiting coronavirus infection.

Conclusions We established the porcine intestinal organoid mucus monolayer as a novel and valuable model for confirming the pivotal role of the small intestinal mucus layer in combating pathogen invasion. In addition, our findings highlight the significance of sialic acid modification of Muc2 in blocking coronavirus infections. This discovery opens promising avenues for the development of tailor-made drugs aimed at preventing porcine enteric coronavirus invasion.

Keywords Coronavirus, Intestinal organoid monolayer, Air–liquid interface (ALI), Mucus layer, Muc2, Sialic acid

†Ning Yang and Yang Li contributed equally to this work.

*Correspondence:
Guangliang Liu
LiuGuangliang01@caas.cn
Full list of author information is available at the end of the article

Background

Coronaviruses, positive-sense enveloped RNA viruses, consist of four genera (α, β, γ, and δ), which cause several pandemic and deadly threats in humans and animals [1]. In piglets, transmissible gastroenteritis virus (TGEV) and porcine epidemic diarrhea virus (PEDV) are major enteropathogenic coronaviruses that are responsible for severe watery diarrhea and result in a huge economic loss in the global pig industry [2, 3]. Although a large number of investigations have focused on the prevention and control of swine enteric coronavirus, there are still no completely effective protective strategies against coronavirus infection [4, 5]. Due to the enteric tropism of TGEV and PEDV, it is crucial to study the antiviral mechanism of the intestinal epithelial barrier to control coronavirus infection.

The intestinal epithelial barrier, which is composed of the mucus layer and intestinal epithelium, plays a critical role in maintaining intestinal homeostasis [6, 7]. Serving as the gatekeeper of the intestinal barrier, the mucus layer coats the apical surface of the intestinal epithelium. It provides not only lubrication for the intestinal contents but also a primary defense line. This is achieved through a hydrated gel-like network that limits the exposure of the underlying epithelial cells to commensal microbes and invading pathogens [8]. The composition of the intestinal mucus mainly includes glycosylated mucins secreted by goblet cells, antibacterial mediators released by Paneth cells and goblet cells, antibodies, and galectins [9]. Muc2 is a major component of mucus in the gastrointestinal (GI) tract. It consists of a core domain called the PTS sequence that is composed of the residues proline (Pro), threonine (Thr), and serine (Ser) repeatedly. During the synthesis of Muc2, the PTS domain undergoes O-linked glycosylation, a modification that results in the formation of a 'bottle brush-like' structure, where the glycan chains extend outward from the core domain. In addition, O-glycans attached to the core backbone of Muc2 can be further modified by the addition of sialic acid or fucose residues, which create additional sites for interactions with microbes [10–12].

Pathogen invasion typically involves traversing the mucus layer before attaching to underlying epithelial cells, highlighting the crucial role of the intestinal mucus layer in resisting pathogen invasion. To date, several studies have underscored the function of soluble mucin in combating bacterial and viral pathogens. For instance, human gastric mucin displays antimicrobial activity against *helicobacter pylori* infection [13], whereas murine intestinal mucins potently inhibit rhesus rotavirus (RRV) infection [14]. In addition, soluble Muc2 purified from the GI tract attenuates the virulence of *Pseudomonas aeruginosa* infection by interacting with mucin glycans [15], and a deficiency in Muc2 enhances the mortality of *Citrobacter rodentium* infections and susceptibility to colitis [16, 17]. Recent findings revealed that bovine mucins could inhibit the human coronavirus OC43 infection in a concentration- and glycan-dependent manner, with the terminal sialyation of mucin playing a key role in reducing viral infectivity [18]. It is similar that these neutralizing activities of murine intestinal mucins against RRV, which are involved in the cleavage of sialic acid residues from mucin molecules, were reduced after neuraminidase treatment [14]. These studies collectively indicate that intestinal mucins play a significant role in inhibiting the virulence or infectivity of pathogenic microorganisms, and this inhibitory effect may be related to the sialylation of mucin. Previous reports have demonstrated that porcine intestinal mucins significantly inhibit TGEV infection and that porcine Muc2 exerts antiviral activity against PEDV infection [19, 20]. Despite these findings, the mechanisms by which intestinal mucus inhibits TGEV and PEDV infection remain unclear. Notably, many reports have demonstrated the sialic acid-binding activity of swine enteric coronaviruses (SeCoVs) [21, 22]. Therefore, we speculate that the inhibitory effect of porcine intestinal mucus on SeCoVs may be related to its sialylation. However, considering the challenges in collecting intestinal mucus and the risk of contamination, there are still many limitations in the verification of the antiviral effect of intestinal mucus and the analysis of its mechanism. Therefore, developing an ideal in vitro intestinal mucus model is crucial to enable more detailed investigations into the antiviral properties of the intestinal mucus.

In this study, we confirmed that the intestinal mucus isolated from the porcine small intestine has protective effects against TGEV and PEDV infections. To further investigate the influence of small intestinal mucus on coronavirus infection, we developed a differentiated porcine intestinal organoid monolayer capable of secreting mucus under ALI conditions. We compared the composition of the mucus derived from the ALI monolayer and native small intestinal mucus. Further investigation demonstrated that mucus derived from the ALI monolayer hinders TGEV and PEDV invasion. Notably, our findings indicate that Muc2 exerts an antiviral effect on attenuating TGEV and PEDV infection and that the sialylation of Muc2 is a pivotal factor in limiting TGEV and PEDV infection.

Results

Porcine native small intestinal mucus entraps TGEV and PEDV

To investigate the impact of the mucus layer on coronavirus infection, intestinal mucus was isolated from the

porcine small intestine and mixed with TGEV and PEDV at 37 °C for 1 h prior to infection. Subsequently, swine testicular (ST) and Vero–E6 cells were incubated with the virus–intestinal mucus mixture, and samples infected with TGEV or PEDV were collected at 16 h post-infection (hpi) (Fig. 1A). The results obtained from RT-qPCR and western blot indicated significant inhibition of TGEV and PEDV infection following pretreatment with native intestinal mucus (Fig. 1B and D). In addition, immunofluorescence assay (IFA) results and quantitative analysis of infected cells corroborated these findings, demonstrating reduced infectivity after TGEV or PEDV was incubated with the native intestinal mucus (Fig. 1C and E). Taken together, these results suggest that native small intestinal mucus may exert an antiviral function by entrapping the virus during coronavirus infection.

To further elucidate the role of mucus in modulating coronavirus infection, we examined the effect of gastric mucus, which is also composed of polymeric mucins modified with O-linked glycans. For this purpose, commercial porcine gastric mucin bound to sialic acid was incubated with TGEV or PEDV for 1 h before infection. Subsequently, ST and Vero–E6 cells were harvested at 16 hpi (Fig. 1A). The RT-qPCR and western blot results demonstrated that preincubation of TGEV with 50 mg/mL porcine gastric mucin significantly decreased the expression of TGEV N proteins (Fig. 1F). Similarly, pretreatment with PEDV and 25 mg/mL porcine gastric mucin obviously suppressed PEDV infection (Fig. 1G). Overall, commercial native mucins from the porcine stomach restricted coronavirus infection, suggesting that mucin was responsible for the inhibitory effect of mucus on coronavirus infection.

Development of differentiated porcine intestinal organoid monolayer

Considering the challenges associated with the collection of natural intestinal mucus and the potential contamination of bacterial proteins in mucus, it is crucial to develop an intestinal epithelium culture model with a mucus layer for further study of the effect of the intestinal mucus on coronavirus infection. In our previous study, we established a porcine intestinal organoid monolayer comprising various epithelial cell types [23]. However, this monolayer exhibited low differentiation efficiency, especially in goblet cells, enteroendocrine cells, and Paneth cells, which means that the model did not fully simulate the intestinal epithelium in vivo. To address these limitations, we developed advanced organoid monolayer models under submerged and ALI culture conditions, improving upon our initial undifferentiated monolayer (Fig. 2A). To characterize the differentiation of organoid monolayer models, the apical structure of the monolayer was evaluated by scanning electronic microscope (SEM). The SEM images revealed that the undifferentiated organoid monolayer presented sparse and short epithelial microvilli, whereas the differentiated monolayers, especially under ALI conditions, exhibited densely packed microvilli, indicative of enhanced epithelial maturation (Fig. 2B). To further evaluate the differentiation of monolayer, the expression levels of markers specific for the different gut epithelial cell types were measured. In ALI cultures, the expression of Villin, Muc2, CGA, and LYZ was significantly upregulated. Although Muc2 and LYZ expression also slightly increased in the submerged culture, the organoid monolayer showed better differentiation levels in the ALI culture. In addition, Sox9 and PCNA expression were decreased in the submerged monolayer (Fig. 2C and D). Subsequently, immunofluorescence staining of different epithelial subsets further confirmed the superior differentiation of ALI cultures. The results indicated that ALI culture significantly increased the differentiation of epithelial cells, especially absorptive enterocytes (Villin positive), goblet cells (Muc2 positive), Paneth cells (LYZ positive), and enteroendocrine cells (CGA positive). In the submerged monolayer, the differentiation effect was inferior to that in the ALI monolayer (Fig. 2E). Controls for primary antibody specificity included staining with an anti-rabbit secondary antibody conjugated with Alexa Fluor 488 and an anti-mouse secondary antibody conjugated with Alexa Fluor 647, which served to minimize nonspecific staining (Additional file 1: Fig. S1). In addition, the transepithelial electrical resistance (TEER) assay was used to evaluate the epithelial integrity of differentiated organoid monolayers under submerged and ALI conditions. The results indicated that the TEER value initially decreased rapidly until it reached a stable plateau ($>200\ \Omega{\cdot}cm^2$) after 4 days in ALI conditions (Additional file 1: Fig. S2). These findings suggest that the organoid monolayer maintained barrier integrity despite the absence of a culture medium on the apical side. Taken together, these findings indicate that the ALI monolayer possesses better differentiation characteristics than the submerged monolayer does and maintains epithelial integrity.

Differentiated ALI monolayer facilitates mucus secretion

In the differentiated organoid monolayer models, mucus secretion is one of the hallmarks of functional maturation. Therefore, we investigated the transcript expression levels of genes associated with mucus production, including chloride channel accessory 1 (CLCA1), zymogen granule protein 16 (ZG16), and Fc gamma binding protein (FCGBP) [24]. The results demonstrated that the ALI monolayer presented higher expression levels of these genes than the other groups did, suggesting an enhanced

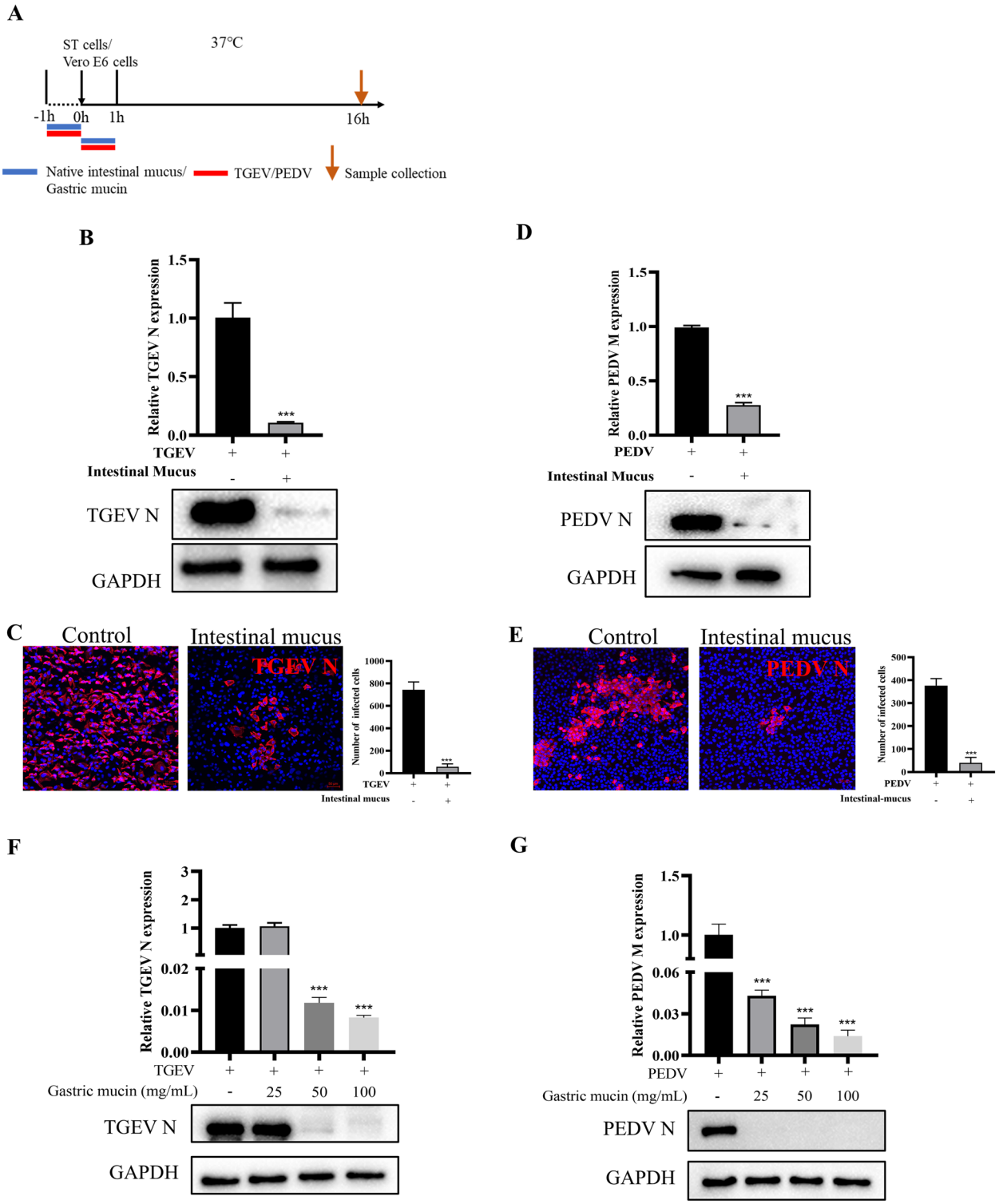

Fig. 1 Porcine native small intestinal mucus entraps TGEV and PEDV. TGEV (MOI = 0.1)/PEDV (MOI = 0.1) was pretreated with 10 μL of porcine intestinal mucus at 37 °C for 1 h. Subsequently, the virus–mucus mixtures were added to ST/Vero–E6 cells and allowed to incubate for 1 h. After infection, the cells were cultured in a fresh medium for 16 h (**A**). The cell samples were collected and analyzed by RT-qPCR and western blot (**B** and **D**). For immunofluorescence staining, the N proteins of TGEV and PEDV were stained in cells incubated with the virus–mucus mixture, and the number of infected cells was quantified by ImageJ (**C** and **E**). The infectivity of TGEV and PEDV in cells treated with the mixture of virus-gastric mucin was evaluated by RT-qPCR and western blot (**F** and **G**). The RT-qPCR data were calculated using the comparative threshold cycle ($2.^{-\Delta\Delta CT}$) method. Results are presented as mean ± SD of data from three independent experiments. *, $P \le 0.05$; **, $P \le 0.01$; ***, $P \le 0.001$

capability for mucus secretion (Fig. 3A). In addition, periodic acid-Schiff (PAS) and Alcian blue (AB) staining, which stains functional goblet cells with glycoproteins and neutral mucins and acid mucins, were performed on sections from different monolayer models. The results showed that the ALI monolayer exhibited more specific staining on the apical side of the monolayer, suggesting that the ALI culture conditions promote the differentiation of goblet cells and mucus production (Fig. 3B). Subsequently, SEM was performed to observe the apical structure of the monolayer. In contrast to the monolayer cultured under submerged conditions, the apical structure of the monolayer cultured under ALI conditions was unclear and covered with a mucus analog when cultured for 6 days, although no visible mucus accumulation was observed on the apical surface at this stage (Fig. 3C). To produce a sufficient amount of mucus for subsequent experiments and detailed characterization, the experiments were extended to 12 days of culture. This extended period resulted in noticeable mucus accumulation on the apical surface of the ALI monolayer (Fig. 3D and E). These results underscore the enhanced mucus secretion capability of the ALI monolayer, indicating its potential as an in vitro mucus model for studying the interaction between the pathogen and the mucus layer.

Mass spectrometry of mucus derived from ALI monolayer

To further evaluate the physiological relevance of the ALI monolayer, we conducted a proteomic analysis to compare the composition of mucus derived from the ALI monolayer with that of native small intestinal mucus. To ensure the reliability of the data, proteins with fewer than one unique peptide were filtered out. Mass spectrometry analysis revealed that a total of 4730 proteins were identified in ALI mucus and 6167 proteins were identified in native small intestinal mucus (the list is presented in the Additional file 2). As shown in Fig. 4A, a total of 2664 proteins were found to be shared between the native small intestinal mucus (SI-M) and ALI-mucus (ALI-M) samples. This significant overlap suggests that the ALI-M closely imitates the composition of native mucus, indicating that the mucus-monolayer model has great potential to replicate multiple biological functions and interactions in the natural gut. On the basis of these 2664 shared proteins, we conducted further screening. Given that epithelial cells are continuously renewed and shed dead cells into mucus, it is reasonable that most identified proteins localize intracellularly. Therefore, to enhance the accuracy of determining the core composition of ALI mucus, we filtered the overlapping proteins on the basis of subcellular localization, considering only those proteins located extracellularly as potential constituents of ALI mucus. Ultimately, 257 proteins were identified as core members of ALI-M (the list is presented in the Additional file 2). According to the Gene Ontology (GO) annotations, these proteins are involved in various biological processes, including macromolecule localization and the regulation of protein metabolic processes (Fig. 4B). In addition, given the intensity-based absolute quantification (IBAQ) results, we compiled a list of the top 20 proteins identified in ALI-M (Table 1). This highlights the major components in mucus derived from the ALI monolayer. Small integral membrane protein 22 (SMIM22), the most abundant protein, may modulate lipid droplet formation in ALI-M. Consistent with the composition of native intestinal mucus, Muc2 was also the primary component in ALI-M, playing a crucial role in forming the mucus gel layer. The list also includes other proteins closely related to intestinal physiological functions. For instance, lysozyme C-3 (LYZ) possesses the major bacteriolytic functions, helping to control microbial populations. Anterior gradient 2 (AGR2) is associated with Muc2 secretion and structural stability and exhibited elevated abundance in ALI mucus. Furthermore, ALI mucus also exhibited a high abundance of proteins with antimicrobial properties, such as regenerating family member 4 (REG4), pentaxin (PTX), and macrophage migration inhibitory factor (MIF). Collectively, the results highlight the similarity between the compositions of ALI mucus and native small intestinal mucus, suggesting that the mucus-monolayer system can provide an ideal model for investigating interactions between mucus and pathogen by closely mimicking the natural environment of the small intestine.

(See figure on next page.)

Fig. 2 Development of differentiated porcine intestinal organoid monolayer. The culture schematic is presented for the development of porcine differentiated intestinal organoid monolayer under submerged and ALI conditions (**A**). SEM observation of the apical structure of epithelial cells in undifferentiated monolayer, submerged monolayer, and ALI monolayer (**B**). Scale bar, 2 μm/1 μm. The expression levels of markers specific for different gut epithelial cell types were analyzed by RT-qPCR and western blot, such as absorption enterocytes (Villin), goblet cells (Muc2), Paneth cells (LYZ), enteroendocrine cells (CGA), stem cells (Sox9) and proliferating cells (PCNA) in undifferentiated monolayer, submerged monolayer and ALI monolayer (**C** and **D**). Immunofluorescence staining of epithelial cell types in undifferentiated monolayer, submerged monolayer, and ALI monolayer, Ki67 also as a marker of proliferating cells (**E**). The RT-qPCR data were calculated using the comparative threshold cycle ($2.^{-\Delta\Delta CT}$) method. Results are presented as mean ± SD of data from three independent experiments. *, $P \le 0.05$; **, $P \le 0.01$; ***, $P \le 0.001$

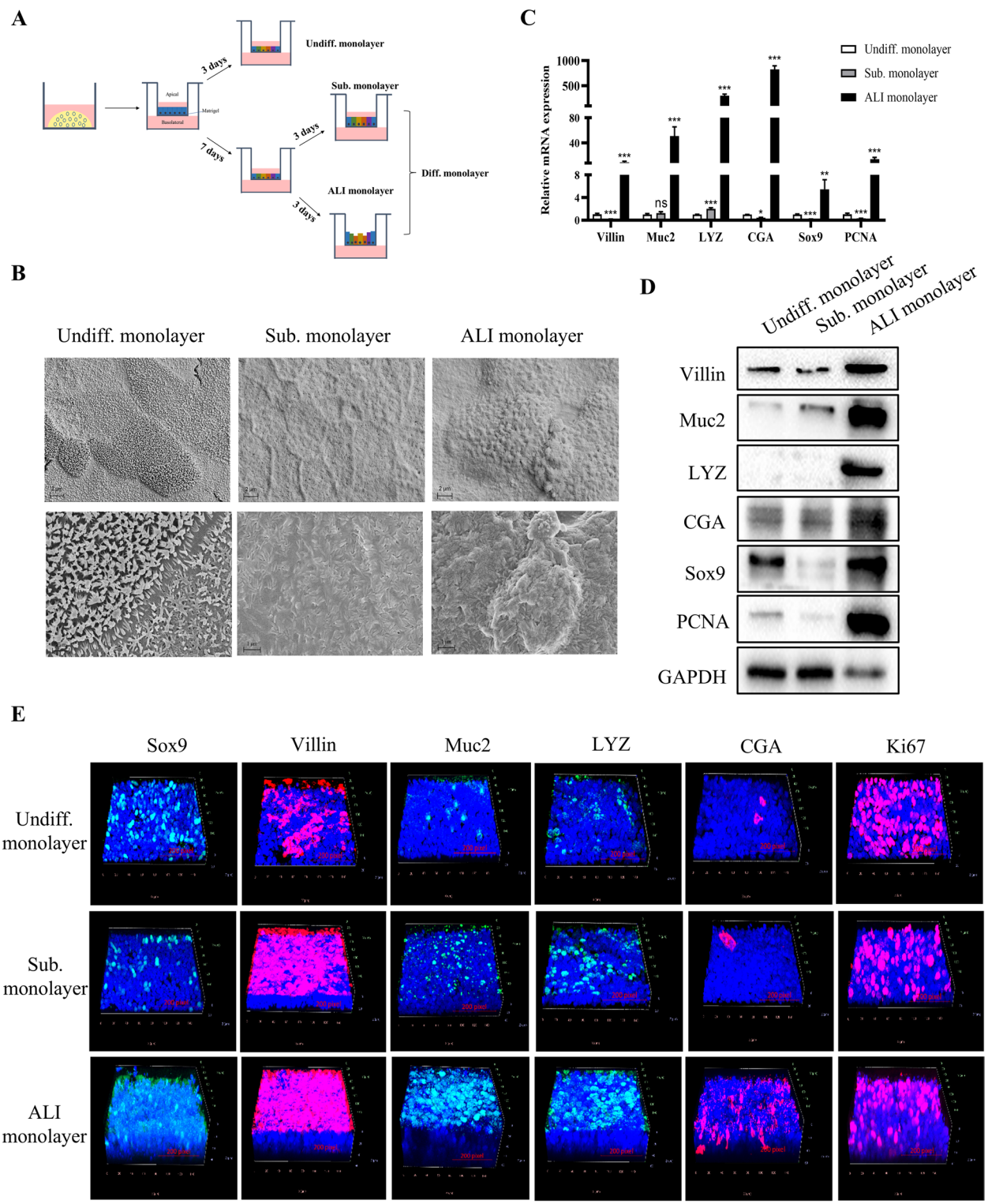

Fig. 2 (See legend on previous page.)

Coronavirus infection is reduced in ALI monolayer

To investigate the characteristics of ALI monolayer enriched with mucus and submerged monolayer on swine enteric coronavirus infection, TGEV and PEDV were employed. The results of the viral load analysis demonstrated that both the submerged monolayer and

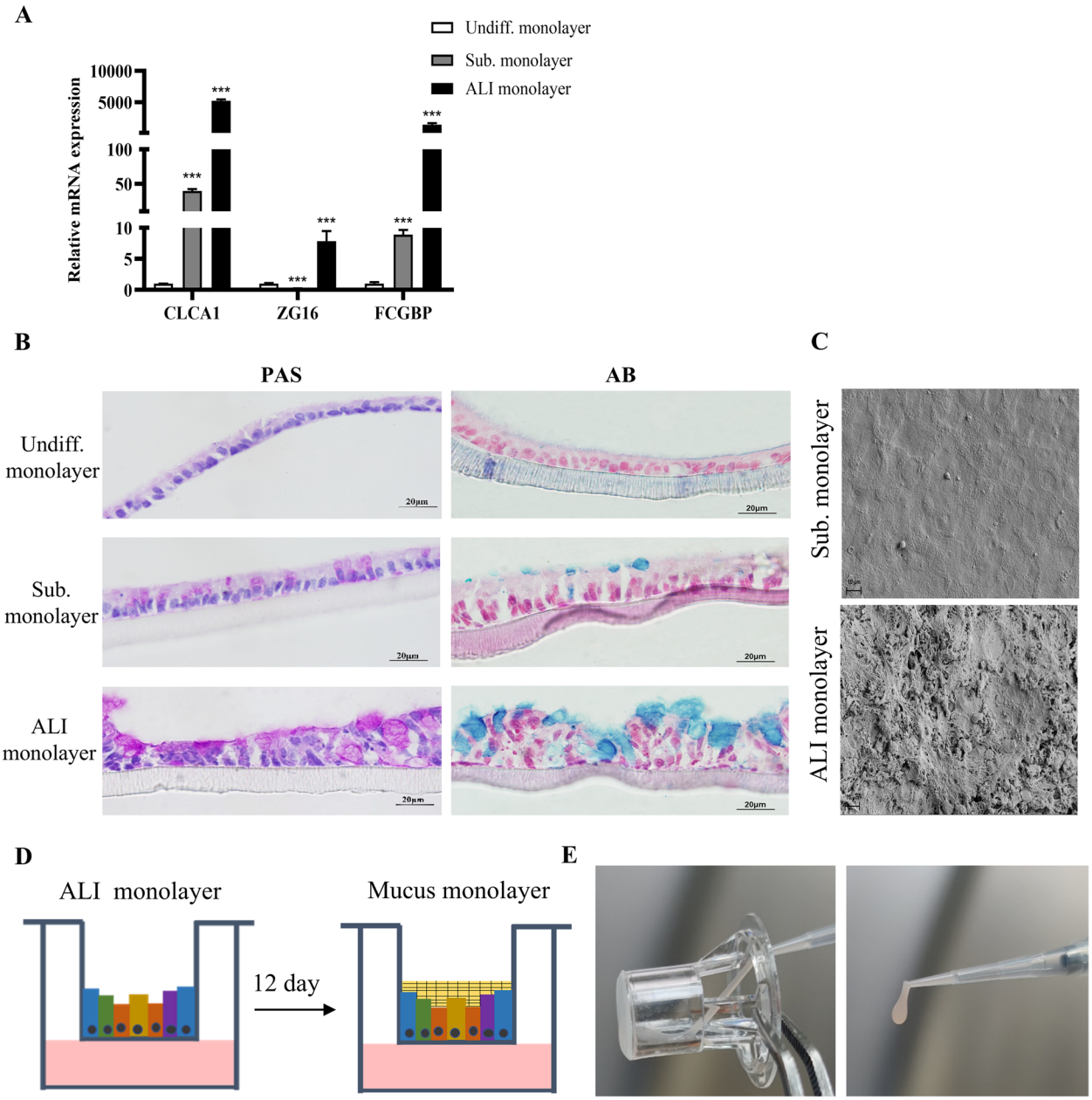

Fig. 3 Differentiated ALI monolayer facilitates mucus secretion. The representative genes associated with mucus secretion were analyzed by RT-qPCR in undifferentiated monolayer, submerged monolayer, and ALI monolayer (**A**). The periodic acid-Schiff (PAS) and Alcian blue (AB) staining were employed to evaluate the differentiation of goblet cells and mucus secretion in undifferentiated monolayer, submerged monolayer, and ALI monolayer (**B**). Scale bar, 20 μm. The apical structure of epithelial cells cultured for 6 days in submerge and ALI condition was scanned by SEM (**C**). Scale bar, 10 μm. Graphical representation for mucus secretion in ALI monolayer (**D**). The hydrated gel mucus from the apical surface of the ALI monolayer was collected (**E**)

ALI monolayer were susceptible to TGEV, but the ALI monolayer showed lower infectivity than the submerged monolayer did (Fig. 5A). Notably, both the submerged monolayer and the ALI monolayer presented a similar viral load at 72 h post-infection, suggesting that the presence of mucus in the ALI monolayer may contribute to the delay in the progression of infection. However, the results of viral titer did not show significant differences, which may be related to the release of virions to both the apical side and the basal side (Fig. 5B). In addition, immunofluorescence staining revealed that the ALI monolayer provides protection against TGEV infection (Fig. 5C and

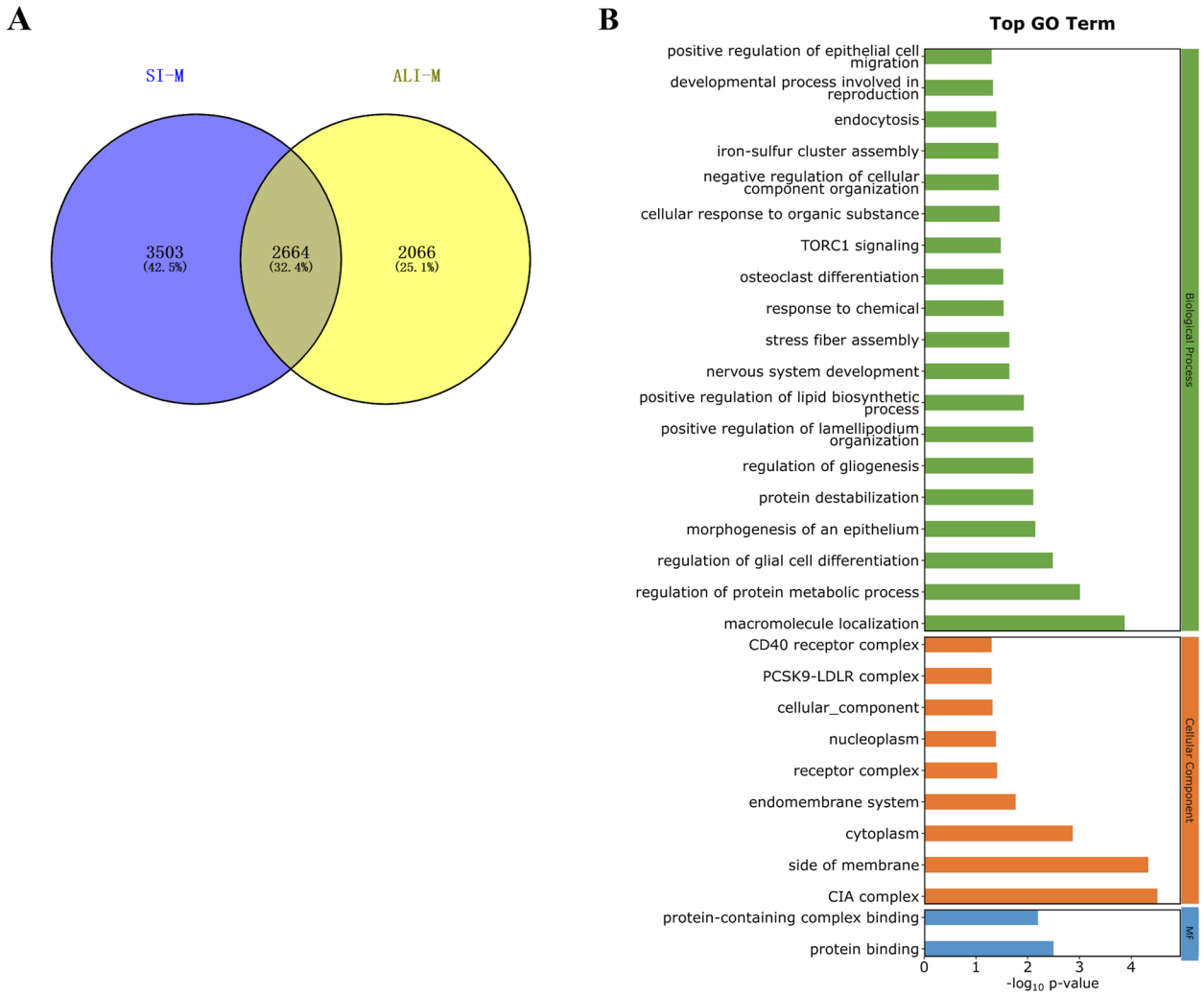

Fig. 4 Mass spectrometry of mucus derived from ALI monolayer. Venn diagram illustrating the overlap in protein identification between mucus derived from ALI monolayer (ALI-M) and native small intestinal mucus (SI-M) (**A**). GO analysis of core composition in ALI-M, categorized by biological process, cellular component, and molecular function (**B**)

D). Although there was no significant difference in the quantitative analysis of the number of infected cells, the ALI monolayer still showed a trend toward low infection. Similarly, low infectivity of PEDV was observed in the ALI monolayer according to the result of RT-qPCR and IFA (Fig. 5E, G and H). Additionally, the PEDV titer in the apical medium supported the protective effect of the ALI monolayer against PEDV infection. Conversely, the result in the basal medium did not support this protection, which may be related to the mucus layer in the ALI monolayer hindering the release of particles toward the cell apex and causing more virions to be released toward the basal side (Fig. 5F). Considering the difference in mucus secretion between the ALI monolayer and submerged monolayer, the low infectivity of the ALI monolayer revealed that the mucus layer may affect the infectivity of TGEV and PEDV when virus passes through the mucus. This hypothesis was consistent with the previous speculation that TGEV and PEDV were trapped after treatment with native intestinal mucus.

Mucus derived from ALI monolayer inhibits TGEV and PEDV infection

To verify the above hypothesis, mucus derived from the ALI monolayer was collected. TGEV and PEDV were preincubated with the ALI mucus at 37 °C for 1 h, respectively. Subsequently, the ST or Vero–E6 cells were incubated with the mixture of virus and ALI mucus, fresh medium was replaced and continued to culture after 1 h incubation, both supernatant

Table 1 Top 20 proteins identified in mucus derived from ALI monolayer

Protein name	Gene	Function	iBAQ
Small integral membrane protein 22	SMIM22	Formation of lipid droplet	3,704,000
Mucin 2	MUC2	Intestinal mucin	3,691,300
Mucin 13B (Fragment)	MUC13B	Transmembrane mucin	3,652,200
Lysozyme C-3	LYZ	Bacteriolytic function	3,574,600
Anterior Gradient 2	AGR2	Required for mucin biosynthesis	3,532,800
GOLD domain-containing protein	TMED10	Protein vesicular trafficking	3,438,900
Regenerating family member 4	REG4	Involved in inflammatory and metaplastic responses of the gastrointestinal epithelium	2,691,900
Glutathione peroxidase	GPX4	Antioxidant peroxidase	2,664,900
Signal sequence receptor subunit delta	SSR4	Regulate the retention of ER resident proteins	2,653,600
Receptor of activated protein C kinase 1	RACK1	Scaffolding protein	2,373,600
Pentaxin	PTX	Regulate innate resistance to pathogens	1,813,400
G Protein Subunit beta 1	GNB1	GTPase activity	1,755,900
Cell division control protein 42 homolog	CDC42	GTP binding protein	1,470,600
Cytochrome c oxidase polypeptide Vb (Fragment)			1,366,700
Thioredoxin	TRX1	Involved in redox reactions	1,237,800
Macrophage migration inhibitory factor	MIF	Pro-inflammatory cytokine involved in the innate immune response to bacterial pathogens	1,111,000
Translocase of outer mitochondrial membrane 40	TOMM40	Mediate the translocation of Complex I components from the cytosol to the mitochondria	1,103,600
ATP synthase protein 8	ATP8	ATP synthase	969,550
Lactamase_B domain-containing protein			900,120
GOLD domain-containing protein	TMED7	vesicular protein trafficking	862,290

and cells were collected at 16 hpi (Fig. 6A). RT-qPCR and $TCID_{50}$ assays were performed to assess TGEV infection, and the results revealed the pretreatment of TGEV with ALI mucus significantly decreased the viral load and release of infectious virus particles (Fig. 6B and C). The result of IFA and western blot further evidenced the decrease in a number of infected cells and expression of TGEV N after TGEV was preincubated with ALI mucus (Fig. 6D, E, and F). Similarly, pretreatment with ALI mucus inhibited PEDV replication and release, as evidenced by RT-qPCR and $TCID_{50}$ assays (Fig. 6H and I). The IFA and western blot results further confirmed a decrease in the number of infected cells and PEDV N expression after treatment with ALI mucus (Fig. 5J, K, and L). To further investigate whether virus particles entrapped in ALI mucus can still be released and infected ST or Vero–E6 cells, we conducted a kinetic experiment with extended incubation periods for mucus–virus cell monolayers. The results demonstrated that prolonged incubation did not significantly impact the inhibition of TGEV or PEDV infectivity by ALI mucus (Additional file 1: Fig. S3). Moreover, the inhibitory effect of ALI mucus on TGEV and PEDV infection was found to be significantly time dependent, as revealed by RT-qPCR and western blotting (Fig. 5G and M). Taken together, our findings suggest that mucus derived from ALI monolayer exerts antiviral activity against coronavirus infections through mucus-virus interactions.

Muc2 inhibits swine enteric coronavirus infection

Given that Muc2 is the primary component of mucus derived from the ALI monolayer and native intestinal mucus. Therefore, we speculated that Muc2 may be

(See figure on next page.)

Fig. 5 Coronavirus infection is reduced in ALI monolayer. The kinetics of TGEV replication were measured by RT-qPCR in the submerged monolayer and ALI monolayer at the indicated time points (**A**). Infectious TGEV particles in the upper chamber medium and lower chamber medium were titrated by $TCID_{50}$ assay (**B**). TGEV N was stained in the submerged monolayer and ALI monolayer by IFA (**C**). The TGEV-positive cell numbers in immunofluorescence staining were quantified by ImageJ (**D**). The kinetics of PEDV replication were measured by RT-qPCR in submerged monolayer and ALI monolayer at indicated time points (**E**). Infectious PEDV particles in the upper chamber medium and lower chamber medium were titrated by $TCID_{50}$ assay (**F**). PEDV N protein was stained in submerged monolayer and ALI monolayer by IFA (**G**). The number of PEDV-positive cells in immunofluorescence staining was quantified by ImageJ (**H**). Results are presented as mean ± SD of data from three independent experiments. *, $P \le 0.05$; **, $P \le 0.01$; ***, $P \le 0.001$

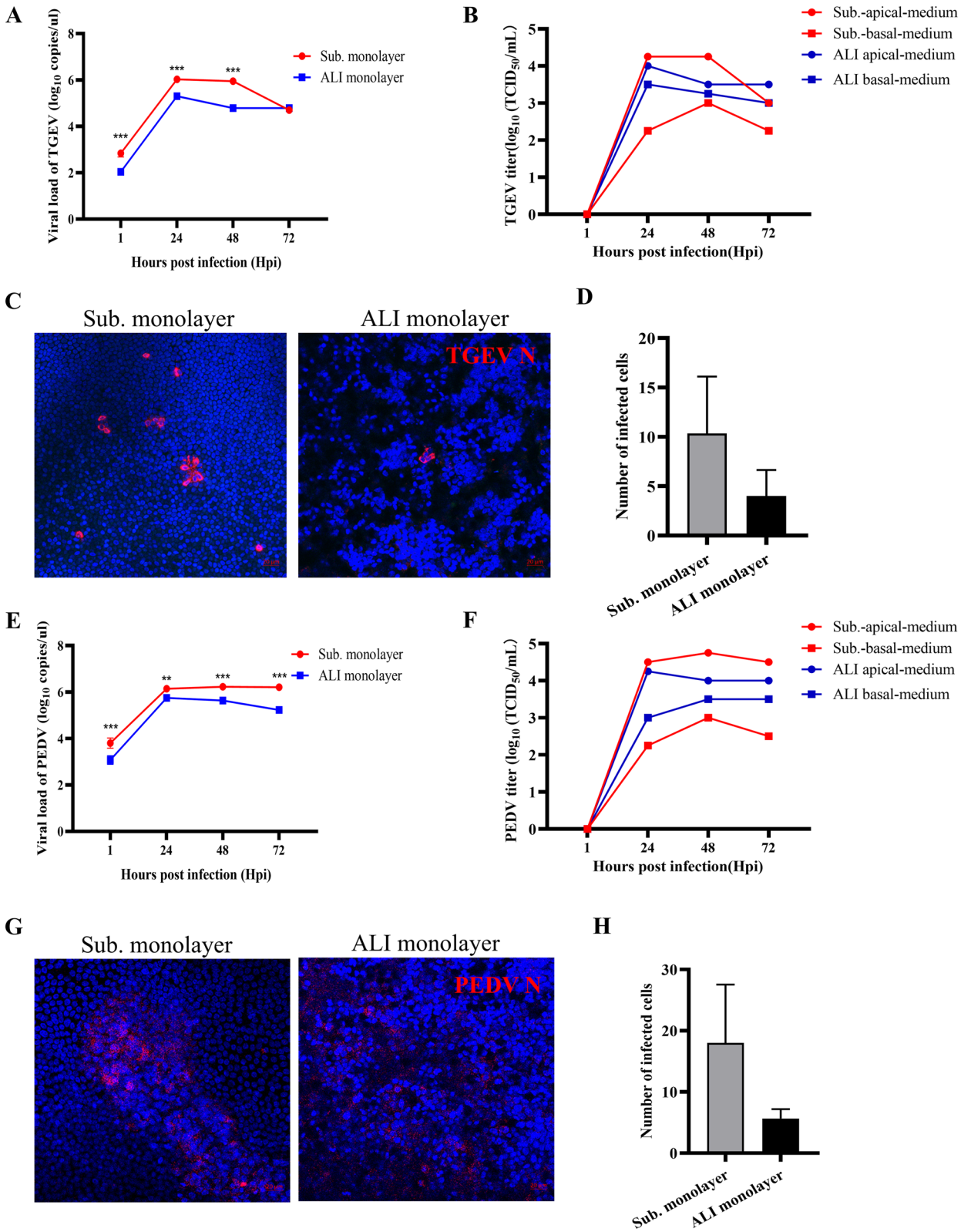

Fig. 5 (See legend on previous page.)

involved in the inhibition of coronavirus infection by mucus. Subsequently, TGEV and PEDV were exposed to recombinant Muc2 produced from *E. coli* (which is not sialylated) and porcine native intestinal Muc2 modified with sialylation for 1 h respectively, and then the mixture was added to ST or Vero–E6 cells, the unattached virus was washed with PBS, and samples were collected at 16 hpi (Fig. 7A). The CCK8 assay illustrated that all tested concentrations of recombinant Muc2 and several concentrations of native Muc2 did not affect cell viability. It is important to note that the results suggested that the highest concentration of native Muc2 can reduce cell viability, but this concentration was not included in the subsequent experimental setup (Fig. 7G and H). In recombinant Muc2 treatment, RT-qPCR and western blot results revealed that the incubation with 50 μg/mL recombinant Muc2 inhibited the TGEV infection, whereas incubation with 12.5 μg/mL recombinant Muc2 reduced PEDV infection (Fig. 7B and C). In the context of native Muc2 treatment, the RT-qPCR and western blot results delineated that pretreatment with 10 μg/mL and 1 μg/mL native Muc2 effectively hindered TGEV and PEDV infection respectively (Fig. 7D and E). The IFA results further displayed the inhibitory effect of native Muc2 on coronavirus infection (Fig. 7F). Collectively, these above findings indicate that Muc2 exerts antiviral activity in inhibiting coronavirus infection through interactions with viruses. In addition, native Muc2 displayed better inhibition in coronavirus infection than did recombinant Muc2.

Sialic acid residues of Muc2 play a potential role in inhibiting swine enteric coronavirus infection

Muc2 secretion is known to undergo O-linked glycosylation modifications, with further modifications including sulfate, sialic acid, or fucose addition. Notably, studies have highlighted that coronaviruses exhibit sialic acid-binding activity during infection [18, 25]. Therefore, we postulated that TGEV and PEDV might bind to Muc2 via sialic acid-mediated interactions. To validate this hypothesis, neuraminidase was employed to cleave sialic acid residues from glycoproteins. Native Muc2 was treated with neuraminidase for 1 h at 37 °C, followed by incubation with TGEV or PEDV prior to infection. Subsequently, the ST or Vero–E6 cells were exposed to the virus–Muc2 mixture for 1 h, and samples were collected at 16 hpi (Fig. 8A). The RT-qPCR and western blot results showed that neuraminidase treatment greatly abolished the inhibitory effect of native Muc2 on TGEV and PEDV infection, especially TGEV infection (Fig. 8B and C). Given that those results were obtained using an attenuated TGEV vaccine strain (TGEV H165), we further investigated the effect of Muc2 sialylation on wild-type TGEV infection using the TGEV Miller strain. The results indicated an obvious reduction in the inhibitory effect of native Muc2 on the TGEV Miller strain following neuraminidase treatment, confirming the consistency of our findings across different viral variants (Additional file 1: Fig. S4). Taken together, these results suggest that the sialic acid modification of Muc2 plays a vital role in its antiviral activity against coronavirus infection, highlighting a potential mechanism by which Muc2 contributes to host defense against enteric viral pathogens.

Discussion

Swine enteric coronavirus causes watery diarrhea, vomiting, and dehydration with high morbidity and mortality in piglets, threatening the pig industry and resulting in enormous economic loss worldwide [1]. To control the epidemic of enteric coronavirus, most studies have focused on the interaction between viruses and epithelial cells. However, the mucus layer that is inseparable from the epithelium is often overlooked due to the difficulties in mucus collection and the lack of a suitable model for studying mucus–host–pathogen interactions. In our study, we addressed this gap by developing a differentiated porcine intestinal organoid monolayer culture system capable of secreting a hydrated gel-like mucus under ALI conditions. This ALI monolayer comprises multiple epithelial cell types and exhibits a high level of differentiation, particularly in goblet cells, enteroendocrine cells, and Paneth cells. To assess the physiological relevance of the mucus produced by the ALI culture, we compared the composition of mucus derived from the ALI monolayer with that of native small intestinal mucus. Our analysis revealed a significant overlap in protein

(See figure on next page.)

Fig. 6 Mucus derived from ALI monolayer inhibits TGEV and PEDV infection. The TGEV (MOI = 0.1)/PEDV (MOI = 0.1) were pretreated with 10 of μL ALI mucus at 37 °C for 1 h, then the mixture was added to the cells and incubated for 1 h respectively, and the cell samples were collected at 16 hpi for detection (**A**). TGEV and PEDV replication was measured by RT-qPCR (**B** and **H**). Infectious TGEV and PEDV particles were quantified by $TCID_{50}$ assay (**C** and **I**). The expression of the TGEV N and PEDV N proteins was detected by IFA (**D** and **J**) and western blot (**F** and **L**). The number of infected cells in immunofluorescence staining was quantified by ImageJ (**E** and **K**). The expression levels of TGEV and PEDV were analyzed by RT-qPCR and western blot at indicated incubation time following treatment with ALI mucus (**G** and **M**). The RT-qPCR data were calculated using the comparative threshold cycle ($2.^{-\Delta\Delta CT}$) method. Results are presented as mean ± SD of data from three independent experiments. *, $P \le 0.05$; **, $P \le 0.01$; ***, $P \le 0.001$

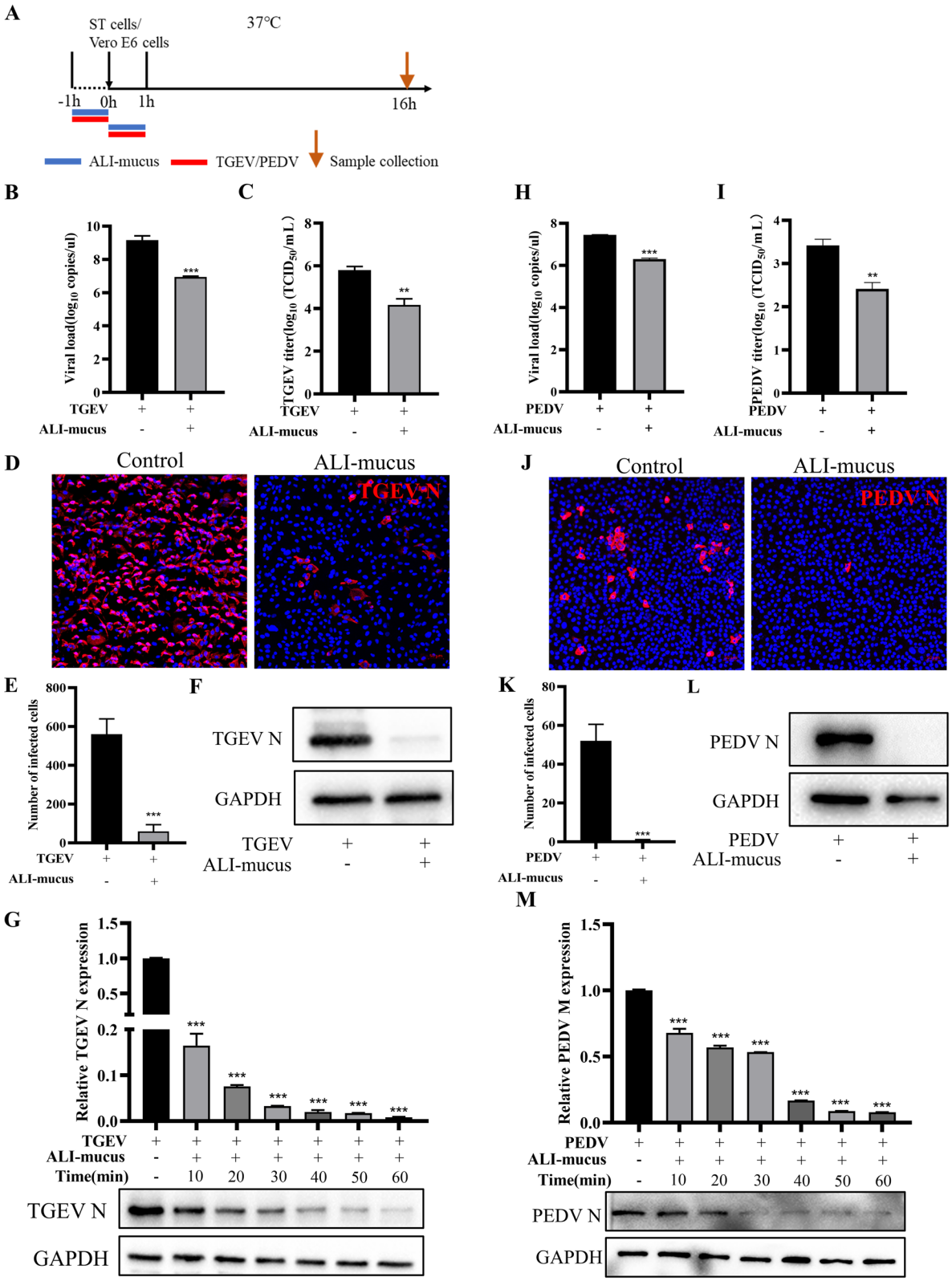

Fig. 6 (See legend on previous page.)

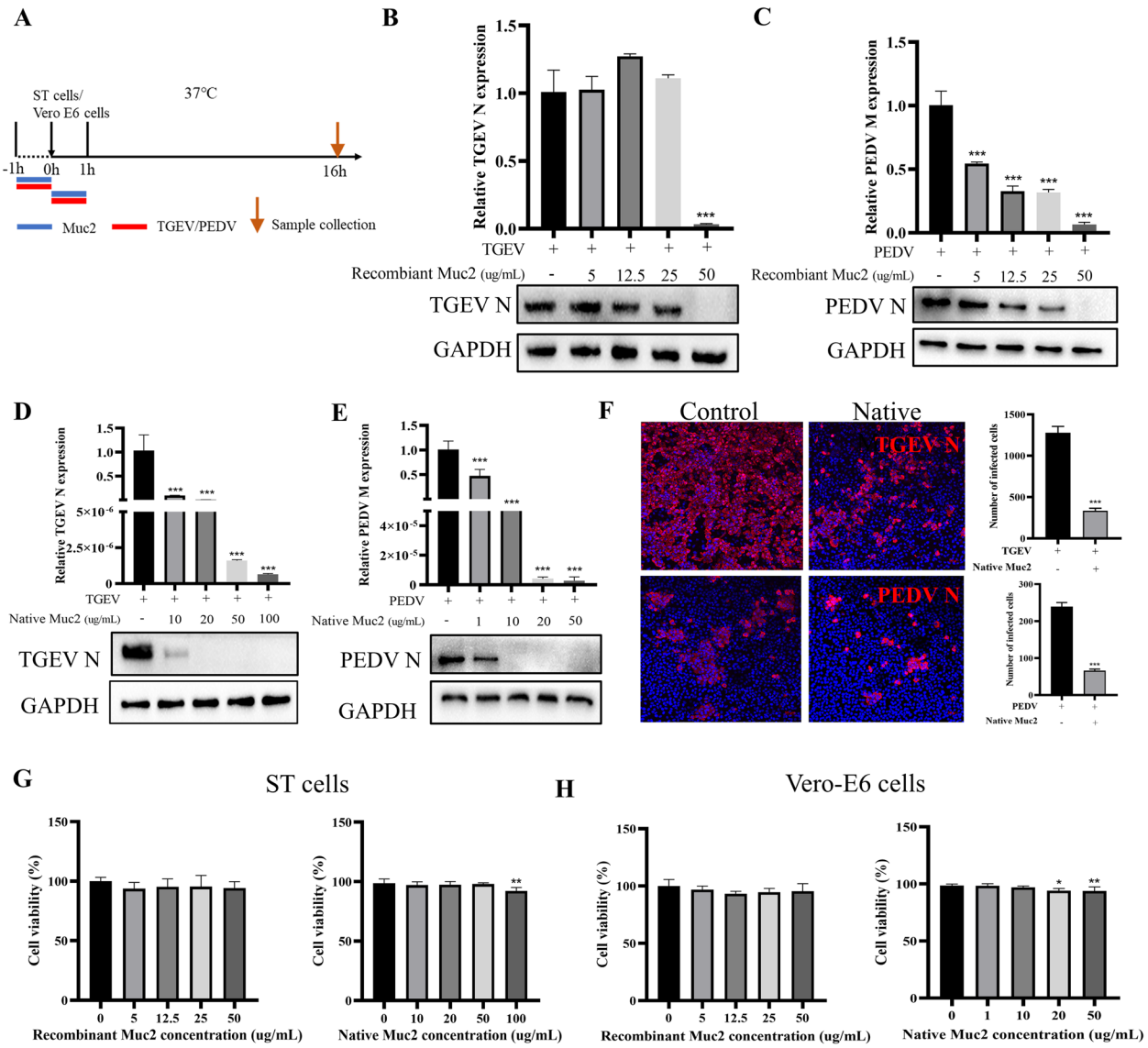

Fig. 7 Muc2 inhibits swine enteric coronavirus infection. TGEV (MOI = 0.1)/PEDV (MOI = 0.1) were pretreated with recombinant Muc2 or porcine native Muc2 of different concentrations at 37 °C for 1 h. Then the mixture was added into ST/Vero-E6 cells for 1 h. The cells were cultured for 16 h (**A**). The expression levels of TGEV and PEDV after treatment with different concentrations of recombinant Muc2 were analyzed by RT-qPCR and western blot (**B** and **C**). The expression levels of TGEV and PEDV after treatment with different concentrations of native Muc2 were analyzed by RT-qPCR and western blot (**D** and **E**). IFA was employed to detect viral protein expression in the cells after treatment with 20 μg/mL native Muc2 in TGEV infection or 10 μg/mL native Muc2 in PEDV infection (**F**). Scale bar, 50 μm. The RT-qPCR data were calculated using the comparative threshold cycle ($2.^{-\Delta\Delta CT}$) method. Results are presented as mean ± SD of data from three independent experiments. *, $P \le 0.05$; **, $P \le 0.01$; ***, $P \le 0.001$

composition between these two sources, indicating that the mucus derived from ALI monolayer effectively replicates key components of the small intestinal mucus environment. This similarity suggests that the ALI mucus has the potential to mimic the physiological properties of native small intestinal mucus, making it a valuable model for studying mucus function.

Some studies have revealed the role of the mucus layer in commensal and pathogenic bacteria invasion via mucus–monolayer systems, such as *enteropathogenic E. coli*, *Lactobacillus rhamnosus*, and *Helicobacter pylori* [24, 26, 27]. In our study, to accurately validate the function of the intestinal mucus layer in SeCoVs invasion, we compared the infection dynamics of viruses in ALI monolayer and submerged monolayer. Our findings

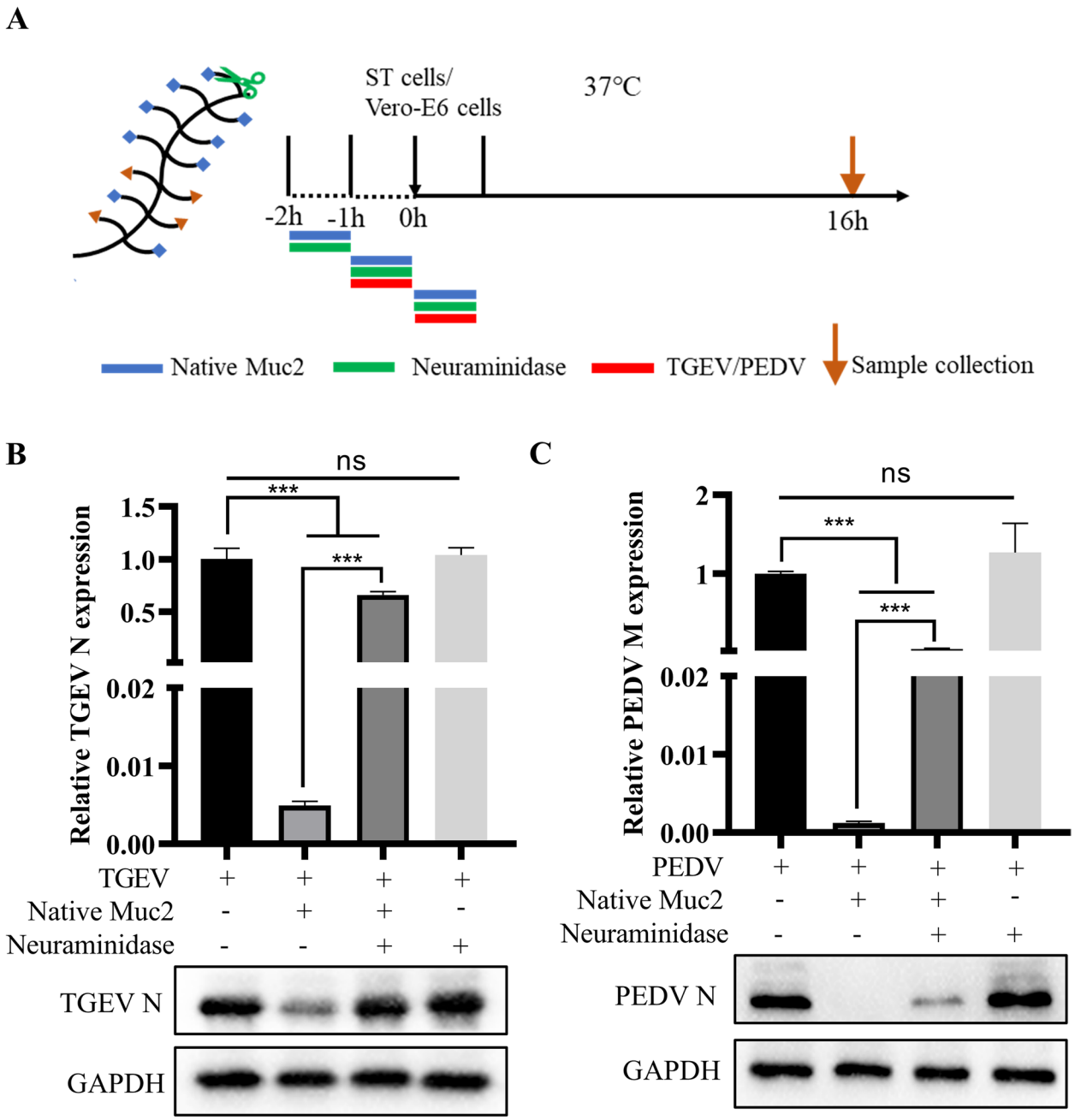

Fig. 8 Sialic acid residues of Muc2 play a potential role in inhibiting swine enteric coronavirus infection. The 10 μg/mL or 1 μg/mL native Muc2 was pretreated with 100 mU of neuraminidase for 1 h at 37 °C. The mixture was incubated with TGEV (MOI = 0.1) or PEDV (MOI = 0.1) respectively prior to infection for 1 h. The cells were harvested at 16 hpi for detection (**A**). The expression of the TGEV N and PEDV M was measured by RT-qPCR (**B**, **D**), and the expression of viral N protein was detected by western blot (**C**, **E**). The RT-qPCR data were calculated using the comparative threshold cycle ($2.^{-\Delta\Delta CT}$) method. Results are presented as mean ± SD of data from three independent experiments. *, $P \le 0.05$; **, $P \le 0.01$; ***, $P \le 0.001$

indicate that the ALI monolayer significantly reduced the infectivity of TGEV and PEDV, which was evidenced by lower viral load and viral protein. However, there was no significant difference in viral titer. Notably, the submerged monolayer released more virions from the apical side than did the ALI monolayer. Conversely, the ALI monolayer exhibited a higher release of virions into the basal medium. This discrepancy may be attributed to the presence of a mucus layer on the surface of the ALI monolayer, which likely impedes the release of viral particles

to the apical surface. Overall, these results suggest that the ALI monolayer provides an effective platform for investigating the role of the mucus layer in SeCoVs invasion and that the mucus layer may hinder both initial contact and subsequent release of viral particles from epithelial cells.

Gel-like mucin is the main component of mucus and makes up the skeleton of the mucus layer [11]. In the case of the porcine intestinal mucus layer, previous studies have shown that TGEV infectivity is inhibited by porcine intestinal mucin [19]. On the basis of these findings, we isolated and investigated the impact of native small intestinal mucus and mucus produced by the ALI monolayer on TGEV and PEDV infection. We found that pretreating the virus with mucus significantly inhibited the TGEV and PEDV infection in a time-dependent manner. This finding not only confirms the inhibitory effect of intestinal mucin on SeCoVs infection but also underscores physiological similarity between mucus derived from ALI monolayer and native mucus. These results further highlight the potential of the ALI monolayer as an effective in vitro model for investigating the interaction between mucus and pathogens.

In accordance with previous findings, Muc2 is a major mucin present in native small intestinal mucus [28]. Similarly, our mass spectrometry analysis confirmed that Muc2 was the principal component in mucus derived from the ALI monolayer. Furthermore, recent research has suggested that Muc2 isolated from porcine intestinal mucus possesses antiviral activity against PEDV infection [20], although the underlying mechanism remains elusive. Therefore, we investigated whether Muc2 also exerts an inhibitory effect on TGEV infection and explored the underlying mechanisms of its antiviral activity. Our study confirmed that Muc2 treatment effectively inhibited TGEV and PEDV infection. Given the unique structure and modifications of Muc2, we propose two potential mechanisms for its antiviral activity against coronaviruses. One possibility is that Muc2 forms a geometric constraint that physically blocks virus infection. We verified this hypothesis by demonstrating that recombinant Muc2 hampered TGEV and PEDV infection. This theory is also supported by previous findings that the shielding effects of biopolymer matrices possess broad-spectrum antiviral properties [29]. Another possible mechanism involves the biochemical interactions that occur due to the sialic acid modifications on Muc2 during its secretion process. Sialic acid is a monosaccharide serving as the terminal ends of O-linked glycoproteins in mucin structures [30]. Sialic acid binding activity with coronavirus spikes has been reported in several coronavirus infections, such as β coronavirus SARS-CoV-2 [31], HCoV-OC43 [32] and BCoV [33], γ coronavirus IBV [34], and α coronavirus TGEV [21], PEDV [22]. Therefore, we investigated the effects of sialic acid residue of Muc2 on TGEV and PEDV infection. We found that the enzymatic removal of sialic acid residues from porcine native Muc2 reversed their inhibitory effect on TGEV and PEDV, suggesting that the sialylation of Muc2 plays a crucial role in blocking coronavirus infection. These findings provide promising strategies for preventing virus invasion by promoting Muc2 secretion or developing tailor-made drugs related to sialic acid residues.

Finally, while the mucus derived from ALI monolayer model effectively mimics the physiological properties of the native intestinal mucus by sharing similar protein components, it does not perfectly match the composition of the native intestinal mucus and replicates the complexity of the intestine in vivo. Therefore, in future research, to improve the accuracy and relevance of the intestinal mucus model, we must comprehensively consider the impacts of diversity and concentration of mucus components. In addition, given the complex composition of the intestinal mucus, there are still lots of potentially active molecules involved in protection against coronavirus invasion. For instance, a recent report showed that calpain-1 purified from porcine small intestinal mucus plays an antiviral activity on PEDV infection [20]. Our mass spectrometry results also mentioned other molecules potentially associated with antiviral activity, such as REG4, PTX, and receptor for activated C kinase (RACK1). Therefore, the specific mechanism by which the intestinal mucus protects against coronavirus invasion still needs further investigation.

Conclusions

Our study successfully established a differentiated porcine intestinal organoid ALI monolayer equipped with a mucus layer. Mass spectrometry analysis further revealed that the composition of mucus derived from the ALI monolayer was similar to that of native small intestinal mucus. This validation underscores the ALI monolayer as a valuable and physiologically relevant model for studying the functions of the mucus layer in intestinal infections. In addition, our findings further demonstrated that the ALI monolayer offers protection against PEDV and TGEV infections, which is related to the role of mucus layer and even intestinal Muc2 in exerting antiviral effects in coronavirus infection. Importantly, sialic acid modification played a crucial role in the antiviral activity of Muc2 against TGEV and PEDV infection (Fig. 9). Collectively, our study developed a novel in vitro model of porcine intestinal mucus, providing a promising tool for investigating the intricate mechanisms underlying

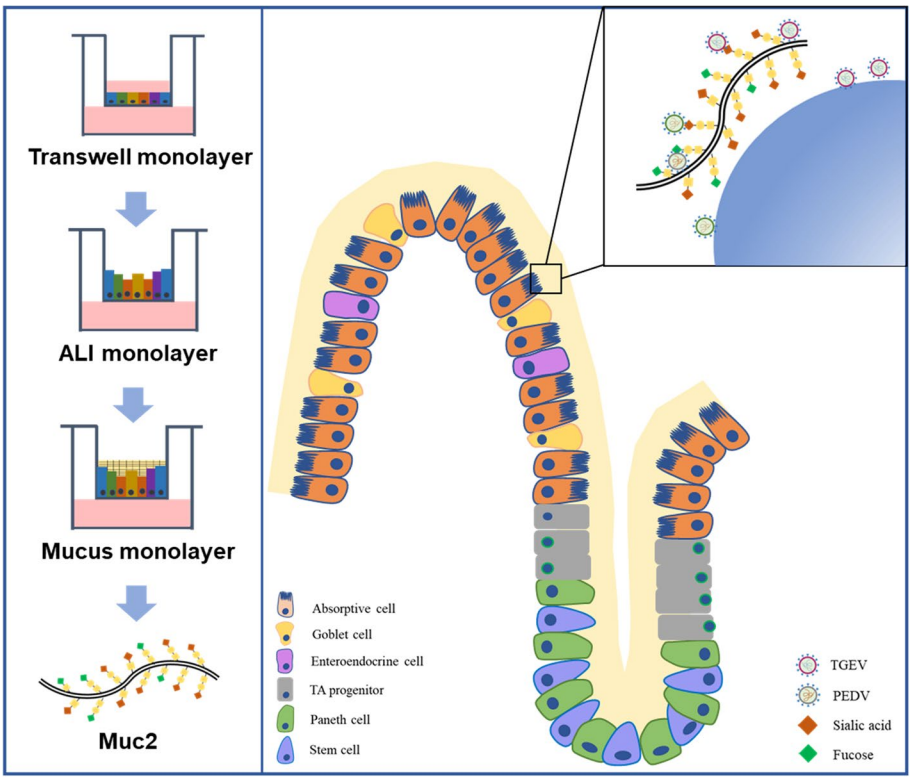

Fig. 9 Schematic diagram of attenuation of swine enteric coronavirus infection by porcine intestinal Muc2 via interactions with sialic acid-linked glycans

intestinal barrier defense against enteropathogenic microorganisms.

Methods

Antibodies

Mouse anti-chicken Villin monoclonal antibody (sc-58897) and mouse anti-human CGA monoclonal antibody (sc-393941) were purchased from Santa Cruz (Texas, USA). Rabbit anti-human Sox9 monoclonal antibody (82630) and mouse anti-PCNA monoclonal antibody (2586S) were purchased from Cell Signaling Technology (Massachusetts, USA). Rabbit anti-human Muc2 monoclonal antibody was purchased from Abcam (ab134119, Cambridge, UK). Rabbit anti-human LYZ polyclonal antibody was purchased from Invitrogen (PA5-16668, California, USA). Mouse anti-human Ki67 monoclonal antibody was purchased from BD Biosciences (550609, New Jersey, USA). Rabbit anti-GAPDH polyclonal antibody was purchased from Proteintech (10494–1-AP, Chicago, USA). TGEV N was kindly gifted by Prof. Li Feng from Harbin Veterinary Research Institute, Chinese Academy of Agricultural Sciences. PEDV N was made in our laboratory. All antibodies were diluted, with a 100-fold dilution applied for IFA and a 1000-fold dilution used for western blot analysis.

Viruses and animals

The TGEV H165 strain was previously recovered from a commercialized attenuated live vaccine and stored in our laboratory (170041133, Keqian Biology, Wuhan, China). TGEV-Miller strain was kindly gifted by Prof. Zhenhui Song from the Department of Veterinary Medicine at Southwest University in Chongqing, People's Republic of China. The cell-adapted PEDV-LJX strain was obtained from diarrheal piglets from a pig farm in Liujiaxia, Gansu province. Briefly, to isolate the virus, the intestinal contents from diarrheal piglets were collected and resuspended in PBS. After centrifugation, the supernatant was collected and filtered through a 0.45-μm filter. We employed TaqMan probe-based reverse transcription–quantitative PCR (RT–qPCR) to screen for several enteric viruses following a previously established protocol in our laboratory [35]. The results indicated a high number of PEDV copies, whereas no other enteric viruses were detected. The supernatant was preserved in -80 °C until further use. For the isolation of crypts and collection of intestinal mucus, porcine ileum samples were obtained

from the Luoniushan slaughterhouse in Hainan Province. The pigs were 6-month-old fattening boars of the Large White breed and were fed with commercial feed. All experimental procedures and animal care were conducted in accordance with the approved guidelines for the Care and Use of Laboratory Animals of Lanzhou Veterinary Research Institute (LVRI), Chinese Academy of Agricultural Sciences, China.

Cell lines culture

ST cells were cultured in Dulbecco's Modified Eagle's Medium (DMEM; D6429, Sigma, St. Louis, USA) supplemented with 10% fetal bovine serum (FBS; A6901, Invigentech, Nova Lima, Brazil), which are commonly used cell lines for TGEV infection. Vero–E6 cells were also cultured in DMEM with 10% FBS, which are widely recognized as ideal cell lines for investigating PEDV infection.

Establishment of mature porcine intestinal organoid monolayer

The generation of porcine ileum organoids and development of organoid monolayer was performed following previous protocols [23, 36]. In brief, 0.33cm^2 transwell inserts (3413, Corning, NY, USA) were incubated with 0.1% Matrigel (356,231, Corning, NY, USA) in DMEM/F12 (D8437, Sigma, St. Louis, USA) for 1 h at room temperature. After aspiration of the liquid, the transwell inserts were air–dried for 15 min. Organoids cultured for 5 days were collected and digested into single cells, after which 150,000 cells were seeded into the precoated transwell. Undifferentiated monolayer was maintained with 200 μL of IntestiCult™ Organoid Growth Medium for humans (OGM; 06010, Stem Cell, Vancouver, Canada) supplemented with 10 μM ATP-competitive inhibitor of Rho-associated kinases (Y-27632; 72,302, CST, MA, USA) in the apical chamber and 500 μL of the same medium in basolateral chamber, and cultured for a duration of 3 days. In addition, for differentiated monolayer, OGM supplemented with Y-27632 was required continuously for 7 days, fresh medium was replaced every two days, and then the medium was switched to IntestiCult™ Organoid Differentiation Medium for human (ODM; 100–0214, Stem Cell, Vancouver, Canada). In submerged monolayer, cells were cultured with ODM containing Y-27632 in both apical and basal chambers. In the ALI monolayer, the medium was thoroughly aspirated from the apical chamber, and ODM containing Y-27632 was added only to the basal chamber. Submerged monolayer and ALI monolayer were cultured for 3 days before the next experiment. For the mucus monolayer, the ALI monolayer generated in the above stage was continued to culture for 12 days, and the medium was replaced every 2 days.

Virus infection

The submerged monolayer and ALI monolayer were washed three times with phosphate-buffered saline (PBS) and subsequently infected with the TGEV H165 strain (MOI = 1) or the PEDV-LJX strain (MOI = 1). Briefly, 68 μL of TGEV of the H165 strain ($10^{6.5}$ $TCID_{50}$/mL) and 12 μL of the PEDV-LJX strain ($10^{7.25}$ $TCID_{50}$/mL) supplemented with 38 μL of DMEM/F12, were added to the apical surface of the transwell for 1 h. The ST or Vero–E6 cell culture supernatants were used to treat the mock-infected organoid monolayers, respectively. The unattached viruses were removed by washing with PBS. The infected organoid monolayers were then cultured with ODM containing 10 mM Y-27632, either under submerged conditions or ALI conditions.

Pretreatment with virus prior to infection

The TGEV H165 strain (MO I = 0.1) or PEDV-LJX strain (MOI = 0.1) was preincubated with native porcine small intestinal mucus (22.21 μg/μL, 10 μL), gastric mucin (M2378, Sigma, St. Louis, USA), ALI mucus (8.22 μg/μL, 10 μL), porcine recombinant Muc2 (RPA705Po01, Cloud-Clone Corp, Wuhan, China) or porcine native Muc2 (NPA705Po01, Cloud-Clone Corp, Wuhan, China) for 1 h at 37 °C respectively. ST or Vero–E6 cells were incubated with the mixture of virus and mucus/Muc2 for 1 h, and then the unattached virus was removed with PBS. The infected cells or supernatants were collected at 16 h post-infection (hpi).

Neuraminidase treatment

The native Muc2 was pretreated with 100 mU neuraminidase (11080725001, Roche, Basel, Switzerland) for 1 h at 37 °C to cleave sialic acid glycans following previous reports [14, 18]. Then the mixture was incubated with the TGEV H165 strain (MOI = 0.1) or the PEDV-LJX strain (MOI = 0.1) for 1 h at 37 °C prior to infection, and a monolayer of ST cells or Vero–E6 cells was infected with the virus–mixture for 1 h at 37 °C, respectively. The infected cells were harvested for detection at 16 hpi.

Virus titration

The infectious virus particles were titrated on ST cells or Vero–E6 cells via the median tissue culture infectious dose ($TCID_{50}$) assay. The cell supernatants were collected at 16 hpi, diluted with tenfold series dilutions, and added to the cells in 96-well plates. Dilutions and wells containing more than 50% cytopathic cells were recorded, and then the virus titration was counted by the Reed-Muench method [37].

RNA extraction and RT-qPCR

The total RNAs from organoid monolayer, Vero-E6 cells, and ST cells were separately extracted using RNAiso reagent (9109, TaKaRa, Kusatsu, Japan). The concentration of the RNA samples was measured using a NanoPhotometer (Implen, Munich, Germany). Subsequently, cDNAs were synthesized using the Honor II 1st Strand cDNA Synthesis SuperMix (R223-01, Vazyme, Nanjing, China) according to the manufacturer's instructions. For viral load detection, the TaqMan probe-based RT-qPCR was employed following the protocol previously established in our laboratory [35]. Relative gene expression levels were performed with 2 × SYBR green master mix (Q311-02, Vazyme, Nanjing, China) according to the manufacturer's instructions. The qPCR parameters were 95 °C for 30 s for initial denaturation; 40 cycles of 95 °C for 10 s, 60 °C for 30 s, followed by a dissociation curve segment (95 °C, 15 s; 60 °C, 60 s; 95 °C, 15 s). Target gene expression was normalized to GAPDH expression, a commonly used housekeeping gene. The relative fold change of the target gene was calculated with the $2^{-\Delta\Delta CT}$ method. The primers and probes used in this study are listed in Table 2.

Western blot

The cells were lysed and harvested using NP40 lysis buffer (P0013F, Beyotime, Shanghai, China) supplemented with phenylmethylsulfonyl fluorid (PMSF; ST505, Beyotime, Shanghai, China) for 20 min at 4 °C after being washed with PBS. The protein samples (20 μL) were loaded and separated on 10% SDS-PAGE gel and transferred onto polyvinylidene difluoride (PVDF) membrane (10600023, GE, Boston, USA). The membranes were then blocked with 5% skim milk (232100, BD, New Jersey, USA) for 2 h at room temperature to prevent nonspecific binding. Subsequently, the membranes were incubated overnight at 4 °C with specific primary antibodies, which were diluted in 0.05% PBST (1:1000). After primary antibody incubation, the membranes were washed with 0.05% PBST and then incubated with HRP-conjugated anti-rabbit secondary antibody (ZB-2306, ZSBIO, Beijing, China) or HRP-conjugated anti-mouse secondary antibody (AP160P, Sigma, St. Louis, USA) for 1 h at room temperature, which were diluted in 0.05% PBST (1:5000). Finally, the protein expression was visualized with chemiluminescence detection reagents (K-12045-D50, Advansta, CA, USA).

Table 2 Primers for real-time qPCR

Names	Primer or probe	Sequence (5′-3′)
Villin	Forward	TTGTAGCGGAGATGAGCGGGAGA
	Reverse	CGGGGAGTGATGACCAGGGTTTC
Muc2	Forward	GGCTGCTCATTGAGAGGAGT
	Reverse	ATGTTCCCGAACTCCAAGG
LYZ	Forward	GGTCTATGATCGGTGCGAGT
	Reverse	AACTGCTTTGGGTGTCTTGC
CGA	Forward	GACCTCGCTCTCCAAGGAGCCA
	Reverse	TGTGCGCCTGGGCGTTTCTT
Sox9	Forward	CGGTTCGAGCAAGAATAAGC
	Reverse	GTAATCCGGGTGGTCCTTCT
PCNA	Forward	TACGCTAAGGGCAGAAGATAATGC
	Reverse	TGAGATCTCGGCATATA-GTG
CLCA1	Forward	CGATGCAAATGGTCGATACAGCGTA
	Reverse	ATGTCGGGTCTCGGCGGGTT
FCGBP	Forward	AGCAATGACCAAGCCTTCCCTAACG
	Reverse	CAGATTGTCCTCGGAGCATGTCGG
ZG16	Forward	GGAGGAGTCGGTGGTCCAGGTGT
	Reverse	TGCAGGCCAATGGCATCAATAAGG
TGEV N	Forward	TGCCATGAACAAACCAAC GGCACTTTACCATCGAAT
	Reverse	HEX-TAGCACCACGACTACCAAGC-BHQ1*a*
	Probe	
PEDV M	Forward	GATACTTTGGCCTCTTGTGT
	Reverse	CACAACCGAATGCTATTGACG
	Probe	FAM-TTCAGCATCCTTATGGCTTGCATC-TAMRA
GAPDH	Forward	CATCCATGACAACTTCGGCA
	Reverse	GCATGGACTGTGGTCATGAGTC

Immunofluorescence staining

The cells were fixed with 4% paraformaldehyde (P0099, Beyotime, China) for 20 min at room temperature, and the excess fixative was removed by washing with PBS for 3 times. Then the cells were permeabilized with 0.2% Triton X-100 (P0096, Beyotime, Shanghai, China) for 20 min prior to being blocked with 5% BSA (4240, Biofroxx, Frankfurt, Germany) for 1 h at room temperature. Primary antibodies were diluted with PBS (1:100) and incubated at 4 °C overnight. Subsequently, the cells were labeled with Alexa Fluor 488-conjugated anti-rabbit secondary antibody (ab150077, Abcam, Cambridge, UK) or Alexa Fluor 647-conjugated anti-mouse secondary antibody (ab150115, Abcam, Cambridge, UK) for 1 h at room temperature, which were diluted with PBS (1:1000). Finally, the nuclei were stained with with 4′,6-diamidino-2-phenylindole (DAPI; C1002, Beyotime, Shanghai, China). In addition, transwell membranes cut with surgical blades and cell slides were placed on glass slides for imaging. Specific markers were observed via a confocal microscopy (Zeiss LSM 900, Germany).

Periodic acid-Schiff and alcian blue staining

The transwell monolayer was rinsed with PBS and fixed with 4% paraformaldehyde, and then incubated at 4 °C overnight. The filter membrane was cut with a surgical blade after being washed 3 times with PBS, embedded in 1% low-melting agarose solution (ST107, Beyotime, Shanghai, China), and paraffin-embed according to the standard protocol. Periodic acid-Schiff (PAS; C0142S, Beyotime, Shanghai, China) and alcian blue (AB; C0153S, Beyotime, Shanghai, China) staining were performed following the manufacturer's recommended protocols.

Scanning electron microscopy

Transwells were washed with PBS, fixed overnight at 4 °C with 2.5% glutaraldehyde (BL911A, Biosharp, Hefei, China), and then washed with PBS 3 times. The filter membrane was cut with a surgical blade, dehydrated through a gradient ethanol, and finally, replaced with tert-butanol (25725–11-5, Macklin, Shanghai, China). Samples were then dried for 2 h using a critical point drier and sputter-coated with gold for 60 s. Visualization was performed with a Zeiss Sigma FE-SEM microscopy (Carl Zeiss, Germany).

Collection and treatment of mucus

Hydrated gel-like mucus derived from the ALI monolayer was aspirated with 10 μL tips and stored at − 80 °C. Following the previous report, native small intestinal mucus was scraped from the ileum of the pigs, resuspended in PBS (1:3 dilutions) supplemented with 2% penicillin/streptomycin (P4333, Sigma, St. Louis, USA) and 100 mg/mL gentamicin (G3632, Sigma, St. Louis, USA). The mucus mixture was vortexed on ice for 15 min and centrifuged at 12,000 rpm at 4 °C for 20 min [14]. Subsequently, the supernatant was collected and stored at − 80 °C until further use.

Mass spectrometry analysis and protein identification

The mucus derived from the ALI monolayer and native small intestinal mucus isolated from porcine ileum were collected. Mucus samples were resuspended in SDT (4% SDS, 100 mM Tris–HCl, 1 mM DTT, pH 7.6) buffer for protein lysis and extraction. Protein digestion was performed according to filter-aided sample preparation (FASP) procedure by trypsin. Briefly, 40 mM DTT was added to samples and mixed for 45 min at 37 °C at 600 rpm and alkylation with 20 mM iodoacetamide (IAA) for 30 min in darkness. Subsequently, trypsin was added to the samples (the trypsin: protein (wt/wt) ratio was 1:50) and samples were incubated for 15–18 h at 37 °C. Afterwards, the peptides were desalted on C18 cartridges, concentrated by vacuum centrifugation and dissolved in 0.1% (v/v) formic acid. Finally, LC–MS/MS analysis was performed on a timsTOF Pro mass spectrometry (Bruker, Germany) that was coupled to Nanoelute (Bruker, Germany). The MS raw data for each sample were identified and quantified using the MaxQuant 1.6.14 software. Database searches were performed against the Sus Scrofa UniProt protein database with the following parameters: (1) 2 max missed cleavages; (2) fixed modifications: carbamidomethyl (C); (3) variable modifications: oxidation (M). The false discovery rate (FDR) was set to 0.01 for proteins and peptides. For quantification, label-free quantification (LFQ) and intensity-based absolute quantification (iBAQ) were enabled.

Statistical analysis

The data from three independent biological replicates were presented as the means ± standard deviations (SDs). The statistical analysis was performed by one-way analysis of variance (ANOVA) or Student's *t*-test with GraphPad Prism 7 software and are shown as *P* values.

Abbreviations

ALI	Air–liquid interface
TGEV	Transmissible gastroenteritis virus
PEDV	Porcine epidemic diarrhea virus
Muc2	Mucin 2
GI	Gastrointestinal tract
RRV	Rhesus rotavirus
SeCoVs	Swine enteric coronaviruses
ST	Swine testicular
TEER	Transepithelial electrical resistance
CLCA1	Chloride channel accessory 1

ZG16	Zymogen granule protein 16
FCGBP	Fc gamma binding protein
PAS	Periodic acid-Schiff
AB	Alcian blue
SI-M	Small intestinal mucus
ALI-M	ALI-mucus
SMIM22	Small integral membrane protein 22
LYZ	Lysozyme C-3
AGR2	Anterior gradient 2
REG4	Regenerating family member 4
PTX	Pentaxin
MIF	Migration inhibitory factor
RACK1	Receptor for activated C kinase

Supplementary Information

The online version contains supplementary material available at https://doi.org/10.1186/s12915-024-02094-7.

Additional file 1: Figure S1-S4. Fig. S1: The result of control staining, anti-rabbit secondary antibody conjugated with Alexa Fluor 488 (A) and anti-mouse secondary antibody conjugated with Alexa Fluor 647 (B). Fig. S2: Evaluation of epithelial integrity in ALI monolayer and submerged monolayer. Fig. S3: Prolonged incubation analysis of ALI Mucus on TGEV and PEDV infectivity. Fig. S4: Sialic acid residues of Muc2 play a potential role in inhibiting TGEV-Miller infection.

Additional file 2: Mass spectrometry analysis. List 1: Mass spectrometry analysis of SI-M. List 2: Mass spectrometry analysis of ALI-M. List 3: Overlapping proteins (SI-M and ALI-M) on the basis of subcellular localization.

Additional file 3: Original blots.

Acknowledgements
The authors thank Dr. Li Feng from the Harbin Veterinary Research Institute, Chinese Academy of Agricultural Sciences, for providing a TGEV nucleoprotein monoclonal antibody. We also extend our gratitude to Prof. Zhenhui Song from the Department of Veterinary Medicine at Southwest University in Chongqing, People's Republic of China, for providing the TGEV-Miller strain.

Authors' contributions
G.L., N.Y., Y.Z., Y.L1., and Y.F. conceived the project. N.Y., Y.C., Y.L1., and Y.L2. performed the experiments. N.Y., G.L., Y.L1., Y.Z., and C.T. analyzed the data. N.Y. drafted the manuscript. L.W. and G.L. edited the manuscript. All authors read and approved the final manuscript.

Funding
This work was financed by the National Natural Science Foundation of China (U22A20522), Science and Technology Major Project of Gansu Province (22ZD6NA001).

Data availability
All data generated and analyzed in this study are included within the article or supplementary materials. Porcine intestinal organoids are available upon request.

Declarations

Ethics approval and consent to participate
All experimental procedures and animal welfare in this study were approved by and in accordance with the guidelines for the Care and Use of Laboratory Animals of Lanzhou Veterinary Research Institute (LVRI), Chinese Academy of Agricultural Sciences, China.

Consent for publication
Not applicable.

Competing interests
The authors declare that they have no competing interests.

Author details
[1]State Key Laboratory for Animal Disease Control and Prevention, College of Veterinary Medicine, Lanzhou University, Lanzhou Veterinary Research Institute, Chinese Academy of Agricultural Sciences, Lanzhou, China. [2]Molecular and Cellular Epigenetics (GIGA) and Molecular Biology (TERRA), University of Liege, Liège, Belgium. [3]Hainan Key Laboratory of Tropical Animal Breeding and Infectious Disease Research, Institute of Animal Husbandry and Veterinary Medicine, Hainan Academy of Agricultural Sciences, Haikou, China. [4]Nutritional Biology, Wageningen University and Research, Wageningen, The Netherlands. [5]College of Veterinary Medicine, Xinjiang Agricultural University, Urumqi, China.

Received: 8 May 2023 Accepted: 12 December 2024
Published online: 23 December 2024

References

1. Cui J, Li F, Shi ZL. Origin and evolution of pathogenic coronaviruses. Nat Rev Microbiol. 2019;17:181–92.
2. Laude H, Rasschaert D, Delmas B, Godet M, Gelfi J, Charley B. Molecular biology of transmissible gastroenteritis virus. Vet Microbiol. 1990;23:147–54.
3. Jung K, Saif LJ, Wang Q. Porcine epidemic diarrhea virus (PEDV): An update on etiology, transmission, pathogenesis, and prevention and control. Virus Res. 2020;286:198045.
4. Yan Q, Liu X, Sun Y, Zeng W, Li Y, Zhao F, et al. Swine Enteric Coronavirus: Diverse Pathogen-Host Interactions. Int J Mol Sci. 2022;23:3953.
5. Liu Q, Wang HY. Porcine enteric coronaviruses: an updated overview of the pathogenesis, prevalence, and diagnosis. Vet Res Commun. 2021;45:75–86.
6. Martens EC, Neumann M, Desai MS. Interactions of commensal and pathogenic microorganisms with the intestinal mucosal barrier. Nat Rev Microbiol. 2018;16:457–70.
7. Peterson LW, Artis D. Intestinal epithelial cells: regulators of barrier function and immune homeostasis. Nat Rev Immunol. 2014;14:141–53.
8. Pelaseyed T, Bergstrom JH, Gustafsson JK, Ermund A, Birchenough GM, Schutte A, et al. The mucus and mucins of the goblet cells and enterocytes provide the first defense line of the gastrointestinal tract and interact with the immune system. Immunol Rev. 2014;260:8–20.
9. Parrish A, Boudaud M, Kuehn A, Ollert M, Desai MS. Intestinal mucus barrier: a missing piece of the puzzle in food allergy. Trends Mol Med. 2022;28:36–50.
10. Herath M, Hosie S, Bornstein JC, Franks AE, Hill-Yardin EL. The Role of the Gastrointestinal Mucus System in Intestinal Homeostasis: Implications for Neurological Disorders. Front Cell Infect Microbiol. 2020;10:248.
11. Paone P, Cani PD. Mucus barrier, mucins and gut microbiota: the expected slimy partners? Gut. 2020;69:2232–43.
12. McGuckin MA, Linden SK, Sutton P, Florin TH. Mucin dynamics and enteric pathogens. Nat Rev Microbiol. 2011;9:265–78.
13. Kawakubo M, Ito Y, Okimura Y, Kobayashi M, Sakura K, Kasama S, et al. Natural antibiotic function of a human gastric mucin against Helicobacter pylori infection. Science. 2004;305:1003–6.
14. Chen CC, Baylor M, Bass DM. Murine intestinal mucins inhibit rotavirus infection. Gastroenterology. 1993;105:84–92.
15. Wheeler KM, Carcamo-Oyarce G, Turner BS, Dellos-Nolan S, Co JY, Lehoux S, et al. Mucin glycans attenuate the virulence of Pseudomonas aeruginosa in infection. Nat Microbiol. 2019;4:2146–54.
16. Bergstrom KS, Kissoon-Singh V, Gibson DL, Ma C, Montero M, Sham HP, et al. Muc2 protects against lethal infectious colitis by disassociating pathogenic and commensal bacteria from the colonic mucosa. PLoS Pathog. 2010;6: e1000902.
17. Van der Sluis M, De Koning BA, De Bruijn AC, Velcich A, Meijerink JP, Van Goudoever JB, et al. Muc2-deficient mice spontaneously develop colitis, indicating that MUC2 is critical for colonic protection. Gastroenterology. 2006;131:117–29.
18. Wardzala CL, Wood AM, Belnap DM, Kramer JR. Mucins Inhibit Coronavirus Infection in a Glycan-Dependent Manner. ACS Cent Sci. 2022;8:351–60.

19. Schwegmann-Wessels C, Bauer S, Winter C, Enjuanes L, Laude H, Herrler G. The sialic acid binding activity of the S protein facilitates infection by porcine transmissible gastroenteritis coronavirus. Virol J. 2011;8:435.
20 Li Y, Wang X, Zhang E, Liu R, Yang C, Duan Y, et al. Calpain-1: a Novel Antiviral Host Factor Identified in Porcine Small Intestinal Mucus. Bio. 2022;13:e0035822.
21. Schultze B, Krempl C, Ballesteros ML, Shaw L, Schauer R, Enjuanes L, et al. Transmissible gastroenteritis coronavirus, but not the related porcine respiratory coronavirus, has a sialic acid (N-glycolylneuraminic acid) binding activity. J Virol. 1996;70:5634–7.
22. Liu C, Tang J, Ma Y, Liang X, Yang Y, Peng G, et al. Receptor usage and cell entry of porcine epidemic diarrhea coronavirus. J Virol. 2015;89:6121–5.
23. Yang N, Zhang Y, Fu Y, Li Y, Yang S, Chen J, et al. Transmissible Gastroenteritis Virus Infection Promotes the Self-Renewal of Porcine Intestinal Stem Cells via Wnt/beta-Catenin Pathway. J Virol. 2022;96:e0096222.
24. Son YS, Ki SJ, Thanavel R, Kim JJ, Lee MO, Kim J, et al. Maturation of human intestinal organoids in vitro facilitates colonization by commensal lactobacilli by reinforcing the mucus layer. FASEB J. 2020;34:9899–910.
25. Li W, Hulswit RJG, Widjaja I, Raj VS, McBride R, Peng W, et al. Identification of sialic acid-binding function for the Middle East respiratory syndrome coronavirus spike glycoprotein. Proc Natl Acad Sci U S A. 2017;114:E8508–17.
26. Reuter C, Alzheimer M, Walles H, Oelschlaeger TA. An adherent mucus layer attenuates the genotoxic effect of colibactin. Cell Microbiol. 2018;20:e12812.
27. Boccellato F, Woelffling S, Imai-Matsushima A, Sanchez G, Goosmann C, Schmid M, et al. Polarised epithelial monolayers of the gastric mucosa reveal insights into mucosal homeostasis and defence against infection. Gut. 2019;68:400–13.
28. Johansson ME, Ambort D, Pelaseyed T, Schutte A, Gustafsson JK, Ermund A, et al. Composition and functional role of the mucus layers in the intestine. Cell Mol Life Sci. 2011;68:3635–41.
29. Lieleg O, Lieleg C, Bloom J, Buck CB, Ribbeck K. Mucin biopolymers as broad-spectrum antiviral agents. Biomacromol. 2012;13:1724–32.
30. Reily C, Stewart TJ, Renfrow MB, Novak J. Glycosylation in health and disease. Nat Rev Nephrol. 2019;15:346–66.
31. Petitjean SJL, Chen W, Koehler M, Jimmidi R, Yang J, Mohammed D, et al. Multivalent 9-O-Acetylated-sialic acid glycoclusters as potent inhibitors for SARS-CoV-2 infection. Nat Commun. 2022;13:2564.
32. Hulswit RJG, Lang Y, Bakkers MJG, Li W, Li Z, Schouten A, et al. Human coronaviruses OC43 and HKU1 bind to 9-O-acetylated sialic acids via a conserved receptor-binding site in spike protein domain A. Proc Natl Acad Sci U S A. 2019;116:2681–90.
33. Schultze B, Herrler G. Bovine coronavirus uses N-acetyl-9-O-acetylneuraminic acid as a receptor determinant to initiate the infection of cultured cells. J Gen Virol. 1992;73(Pt 4):901–6.
34. Shahwan K, Hesse M, Mork AK, Herrler G, Winter C. Sialic acid binding properties of soluble coronavirus spike (S1) proteins: differences between infectious bronchitis virus and transmissible gastroenteritis virus. Viruses. 2013;5:1924–33.
35. Huang X, Chen J, Yao G, Guo Q, Wang J, Liu G. A TaqMan-probe-based multiplex real-time RT-qPCR for simultaneous detection of porcine enteric coronaviruses. Appl Microbiol Biotechnol. 2019;103:4943–52.
36. Li Y, Yang N, Chen J, Huang X, Zhang N, Yang S, et al. Next-Generation Porcine Intestinal Organoids: an Apical-Out Organoid Model for Swine Enteric Virus Infection and Immune Response Investigations. J Virol. 2020;94:e01006–20.
37. Han N, Chen Z, Wan H, Huang G, Li J, Jin BR. A rapid method for titration of ascovirus infectivity. J Virol Methods. 2018;255:101–6.

Publisher's Note